INTERNATIONAL JOURNAL OF
COASTAL, OFFSHORE & ENVIRONMENTAL ENGINEERING IJCOE Vol.8/No. 1/winter 2023 (1-9)

Available online at: www. Ijcoe.org

Investigating the downwelling of Persian Gulf Water in the Gulf of Oman

Hossein Ramak[1], Maryam Soyuf Jahromi[2*], Akbari, Parastoo[3]

[1] *PhD of physical oceanography, Department of Nonliving Resources of Atmosphere and Ocean, Faculty of Marine Science and Technology, University of Hormozgan, Bandar Abbas, Iran; Department of physics, Education office of Hormozgan Province, Education Ministry, Parsiyan, Iran, hoseynramak@gmail.com*
[2] *Assistant Professor of physical oceanography, Department of Nonliving Resources of Atmosphere and Ocean, Faculty of Marine Science and Technology, University of Hormozgan, Bandar Abbas, Iran, soyufjahromi@yahoo.com.au*
[3] *Department of physics, Education office of Khoozestan Province, Education Ministry, Ahwaz, Iran, pakbari91@yahoo.com*

ARTICLE INFO

Article History:
Received: 26 Dec. 2022
Accepted: 02 Feb. 2023

Keywords:
Water Mass
Seasonal change
Downwelled Water
Vertical Velocity
FVCOM

ABSTRACT

In Gulf of Oman, the sinking of Persian Gulf Water mass has been reported. In the current study, the FVCOM ocean model has been used in 20 layers to investigate the phenomenon of downwelled Persian Gulf Water in the Gulf of Oman. The bathymetry of the simulated area (47˚-59.45˚E, 22˚-32˚N) was achieved from GEBCO-2019 by the resolution of 30 seconds. Triangular grid was generated in SMS. The open boundary fluctuations were also extracted from TMD. The temperature and salinity were obtained from the output of HYCOM (standard depths). Satellite data were used for the verification. The results showed the downward vertical velocity of Persain Gulf Water is higher in the area of the sudden depth change than the other parts in all seasons. This fact indicated the downwelled water was in a form of a spot. The rate of downwards penetration of water was different (winter: -2cm/s, spring: -1cm/s, summer: -1.2cm/s, autumn: -1.7cm/s). In summer, the salinity contours were very close to each other in the east of the Strait of Hormuz, or intense stratification. Therefore, the slope of the salt wedge was less. In winter, the calculated slope of the salt wedge (1.5×10^{-1} degrees) was greater than summer (3.8×10^{-2} degrees). The larger angle or slope of the salt wedge means the greater horizontal component of the weight of water ($mg\sin\theta$). It causes the displacement of saline water, and faster movement of Persian Gulf Water. Therefore, the water of the Persian Gulf moves faster to lower depths in Gulf of Oman in winter than summer.

1. Introduction

Downwelling is the opposite process of upwelling, in which surface water flows downward and replaces deep water. This happens in parts of the ocean where the surface winds are converging. A cyclonic wind causes a decrease in sea level, an increase in the thermocline, the divergence and upwelling, while an anticyclonic wind leads to an increase in the sea level, a lower thermocline, and convergence and downwelling. One of the places where upwelling or downwelling occurs is in the center of the gyres, cycles and eddies even if there is no prevailing wind [1].

Upwelling and Downwelling are two prominent features that appear in an annual cycle on the west coast of India [2-6]. Heat transfer [7] and mass transfer [8] (such as carbon dioxide) from the ocean to the atmosphere and vice versa are key processes that accompany downwelling currents [7]. Even the primary biological production in the eastern Arabian Sea is not only done by the upwelling phenomenon, but can also occur under the influence of the proper downwelling phenomenon caused by Kelvin waves that lower the thermocline [9-12] in the northeast of the Arabian Sea during the northeast monsoon (November-February) [13-14]. Therefore, understanding and studying the phenomenon of downwelling and upwelling is of great scientific importance in designing fisheries management strategies to provide maximum sustainable yield.

It was seen in the northeast of the Arabian Sea that the vertical downwelling of the water causes the heating of the mixing layer waters during winter. Because the vertical velocity of water in these areas is negative, which indicates the phenomenon of downwelling. The simulation showed that the atmospheric currents tend to cool the mixing layer of the Arabian Sea, but this

cooling of the mixing layer is countered by the warming caused by horizontal advection. Downwelling is the tendency to heat the lower layer and reduce or neutralize the rate of cooling of the mixing layer, and it can continue, and even as the mixing layer becomes shallower. This causes the formation of a weak barrier layer under the mixing layer in the south-northeast of the Arabian Sea, which prevents the cooling of this layer [13].

The role of vertical subsidence, which tends to heat the mixing layer and is due to the downwelling phenomenon, has been largely ignored in studies, and more attention has been paid to the upwelling phenomenon. This study aims to investigate the downwelling of Persian Gulf water in the Oman Sea by using numerical simulation, and evaluates the changes of the Persian Gulf water fall in the Gulf of Oman during the seasons.

2. Materials and Methods

2.1. The study area

The Gulf of Oman is a water basin that is located in the northwest of the Arabian Sea, the Indian Ocean, and the east of the Strait of Hormuz and the Persian Gulf, and it is spread in latitude of 22˚N to 26˚N and longitude 56˚E to 60˚E. Iran is located in the north of this gulf and Oman is in the south. The continental slope is sharp in the east of 56˚E and along the coast of Oman. So that the depth of more than 3000 meters is found in the south of 24.30˚N and in the east of 58.30˚E in this gulf [15] (with a maximum depth of 3398 meters [16]). This gulf is located in the warm region of the earth, where the maximum sea surface temperature of 33˚C in August, and the minimum of 19.8˚C in January. It is different from part to parts. The maximum of sea surface temperature anomaly occurs in Auguest [17] in most parts. The tide of the Gulf of Oman is also the same as the tide of the Arabian Sea [16] and is different from Persain Gulf [18] which which affects the region's renewable energies at different points and times [19]. The circulation pattern in this basin includes an outflow from the Strait of Hormuz to a depth of approximately 200 meters, which extends throughout the basin, and the other one is the rotation of clockwise in the west and anti-clockwise in the east [16]. The dominant wind in this region is the south wind in summer and the northwest wind in winter [16]. The direction of wind movement in the Gulf of Oman is associated with seasonal reversal, corresponding to the monsoon system of the Indian Ocean, so that during the winter monsoon (October-May), the northwest wind prevails and during the summer monsoon (June-September), the southeast wind prevails [20].

In order to investigate the water mass of the Persian Gulf in the Gulf of Oman, an area was chosen that includes the Persian Gulf. Hence the study area of this research was located between 22˚N to 32˚N and 47˚E to 59.45˚E, on the north of Arabian Sea.

2.2. The numerical simulation

The FVCOM 3D numerical ocean model of Finite-Volume Coastal Ocean Model version 3.2.1, hereafter FVCOM, is a finite volume model that can provide suitable simulations for ocean projects by discretizing the equations [21] in an unstructured horizontal triangular computational grid [22]. The model has the ability to use sigma coordinates (with uniform or variable resolution from the surface to the bed) in the vertical direction [23]. Hence, the ability to accurately solve the equations by encoding in a Cartesian or spherical coordinate system, while maintaining the scale and topological flexibility provided by the unstructured meshing and the simplicity of the coding structure, has made this model suitable for many coastal and interdisciplinary scientific applications with complicated conditions [23].

2.2.1. Inputs

The initial input files of FVCOM included entering the horizontal computational grid, depth, sigma layer (20 layers), boundary points, sponge layer information and Coriolis meter, water level and initial conditions of temperature and salinity.

First, the data related to the coastline of the studied area was extracted from the GEBCO-2019 database in Shapefile format [24]. The specialized software of Surface-water Modeling System version 10.0 [25-26], hereafter SMS, was used to create an unstructured triangular mesh from the prepared bathymetry data for FVCOM. All three modules Mesh Module, Map Module and Scatter Module of SMS were used to generate the computing grid. After changing the structure in the SMS software environment and creating the ability to smooth the coastline, the necessary corrections were applied to the file, and then an unstructured two-dimensional computing mesh with appropriate resolution was created in different areas of the study area. This mesh of 11136 cells and 5879 nodes with a horizontal resolution between 950 m and 4700 m was used in 20 sigma layers in the vertical direction. The bathymetry data were extracted from GEBCO-2019 data, relative to the mean sea level in meters, with a resolution of 30 seconds [27] and interpolated on the computational grid, so that a depth was assigned to each node of the grid. In different areas of the model, the depths were not the same and there were depths less than 2 meters (1.02 m) and greater than 3000 meters (3256 m) in the Gulf of Oman. In order to investigate the downwelling of the Persian Gulf water in the Gulf of Oman from the Strait of Hormuz towards the Gulf of Oman, a finer grid was used. Figure 1 illustrates the part of the computational fine mesh of Gulf of Oman used in FVCOM.

The information of the sponge layer and the Coriolis parameter were entered into the model as separate ASCII files.

The open boundary was located at 59.45˚E, and the number of points on the open boundary was considered to be 35 nodes. They were also entered into the model as separate ASCII files. The water level, as the main settings of the model, at the open boundry nodes with NetCDF format was extracted from Tidal Model Driver, hereafter TMD, as constant values of the domain in the coordinates corresponding to the location of the nodes of the open boundry of the computing grid with a time step of one hour.

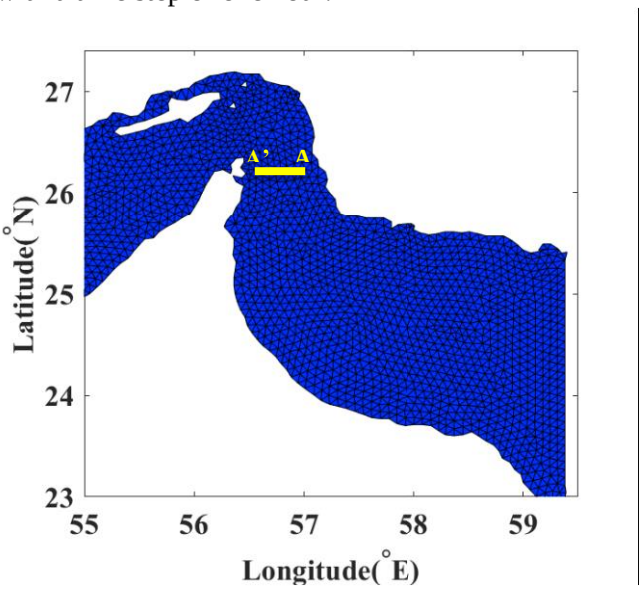

Figure 1: The computational mesh generated by SMS in Gulf of Oman and used for FVCOM simulation. The AA' (yellow line) is a cross section regarding Figures 4 and 6.

The initial conditions of temperature and salinity used in the model were considered non-uniform, and these initial conditions were entered into the model as a NetCDF field of temperature and salinity. Temperature and salinity data fields by a horizontal resolution of 0.08 degrees were used from the HYbrid Coordinate Ocean Model, hereafter HYCOM [28], at standard depths (ten levels of depth).

2.2.2. Outputs

The initial conditions of temperature and salinity used in the model were considered non-uniform, and these initial conditions were entered into the model as a NetCDF field of temperature and salinity. Temperature and salinity data fields by a horizontal resolution of 0.08 degrees were used from the HYbrid Coordinate Ocean Model, hereafter HYCOM [28], at standard depths (ten levels of depth).

The output files included hourly water level and daily salinity, temperature and current, which were prepared in NetCDF format. MATLAB 2016 software [29] with appropriate coding was used to illustrate the outputs of the simulation.

2.2.3. Validation

The simulation had been run for 6 years (from 2014 to 2020) so that the properties of the water mass of Persian Gulf reach a stable cycle.

To validate the results of the simulation, it was used satellite data from the Group for High Resolution Sea Surface Temperature, GHRSST, with the resulation of 0.05˚ and an accuracy of 0.01˚C known as OSTIA [30]. The maximum difference between OSTIA and the simulation was about 1.9˚C (warm season) and 0.7˚C (cold season). In warm season, in most of the Gulf of Oman and its east, the difference was around +0.4˚C, and in the cold season, it was around -0.2˚C to +0.2˚C.

3. Results and Discussion

The results of the numerical FVCOM simulation show the pattern of vertical water velocity during seasons in the Gulf of Oman. Figure 2 shows that in most of the studied range in the deep layers, the velocity is close to zero (green areas), but in some areas, the vertical velocity of water from neutral buoyancy is positive (red dots) and negative (blue spots) which represents rising (upwelled) and sinking (downwelled) water, respectively.

In winter (the first row of figure 2), in the 18th and 19th sigma layers in the southern regions of the Gulf of Oman, the downward vertical velocity of water is higher than in other regions. In the 18th layer, there is a spot with a velocity of -1.2 cm/s and in the 19th layer, the vertical velocity of water in the same areas is -1.8 cm/s. It finally reaches -2 cm/s In addition, in the southern regions of the Gulf of Oman, near the coast of Oman, there is a narrow strip of water with a vertical velocity of -1 cm/s. Therefore, in winter, with the depth increase from the 18th sigma layer to the 20th sigma layer, the downward vertical velocity of water is increasing, so that it has the highest value in the 20th sigma layer.

In spring (the second row of figure 2), the vertical velocity of water in most areas of the Strait of Hormuz and the Gulf of Oman in the 20th sigma layer is in the range of -0.1 cm/s to 0.1 cm/s, and in the central areas of the Gulf of Oman, the vertical water speed is also -0.03 cm/s to -0.5 cm/s. In the east of the Strait of Hormuz, at the longitude of 57.12˚E, the maximum downward vertical velocity can be seen, and its value is about -1 cm/s. In the southern regions of the Gulf of Oman, near the coast of Oman, there is also a strip parallel to the coast, the vertical speed of the water is -1.2 cm/s, and in the eastern regions of the Gulf of Oman, the vertical speed of the water is around -0.3 cm/s to -1.1 cm/s (figure 3, the second row). In the spring, the vertical downward velocity in the 18th and 19th layers of the eastern regions of the study area is higher than in other regions. In the southeastern regions of the Gulf of Oman, the vertical downward velocity reaches -1 cm/s. In the 18th and 19th layers in the Strait of Hormuz and east of it, there is no significant vertical downward velocity, but in the 20th layer and in the east of the Strait of Hormuz, the velocity has increased compared to the above layers.

In summer (the third row of figure 2), the vertical velocity of water in most areas of the Strait of Hormuz and the Gulf of Oman in the 20th sigma layer is in the range of -0.1 cm/s to -0.1 cm/s. In this season, like other seasons in the east of the Strait of Hormoz, the maximum vertical velocity of water is downward and about -2.1 cm/s in the longitude of 57.12 ˚E to 57.26˚E. In the east of the Gulf of Oman and in the range of longitude 59˚E, the downward vertical velocity is higher than in other areas (-1cm/s). In the southern regions of the Gulf of Oman, water with a vertical velocity of -1.8 cm/s covers those regions in a narrow manner (the third row of figure 2). In summer, the downward vertical velocity in the 18th and 19th layers are in the range of -0.8 cm/s to -1 cm/s. In the eastern areas of the Strait of Hormuz, the downward velocity has increased in this season compared to spring. In the east of the Gulf of Oman, the downward vertical velocity increases and its value reaches -1 cm/s. In the south, the speed of -1.5 cm/s can be seen in some areas. From the 18th to the 20th sigma layer, with the increase in depth in this season, the downward vertical velocity has also increased, so that in the 20th sigma layer, the vertical downward velocity is more than other layers.

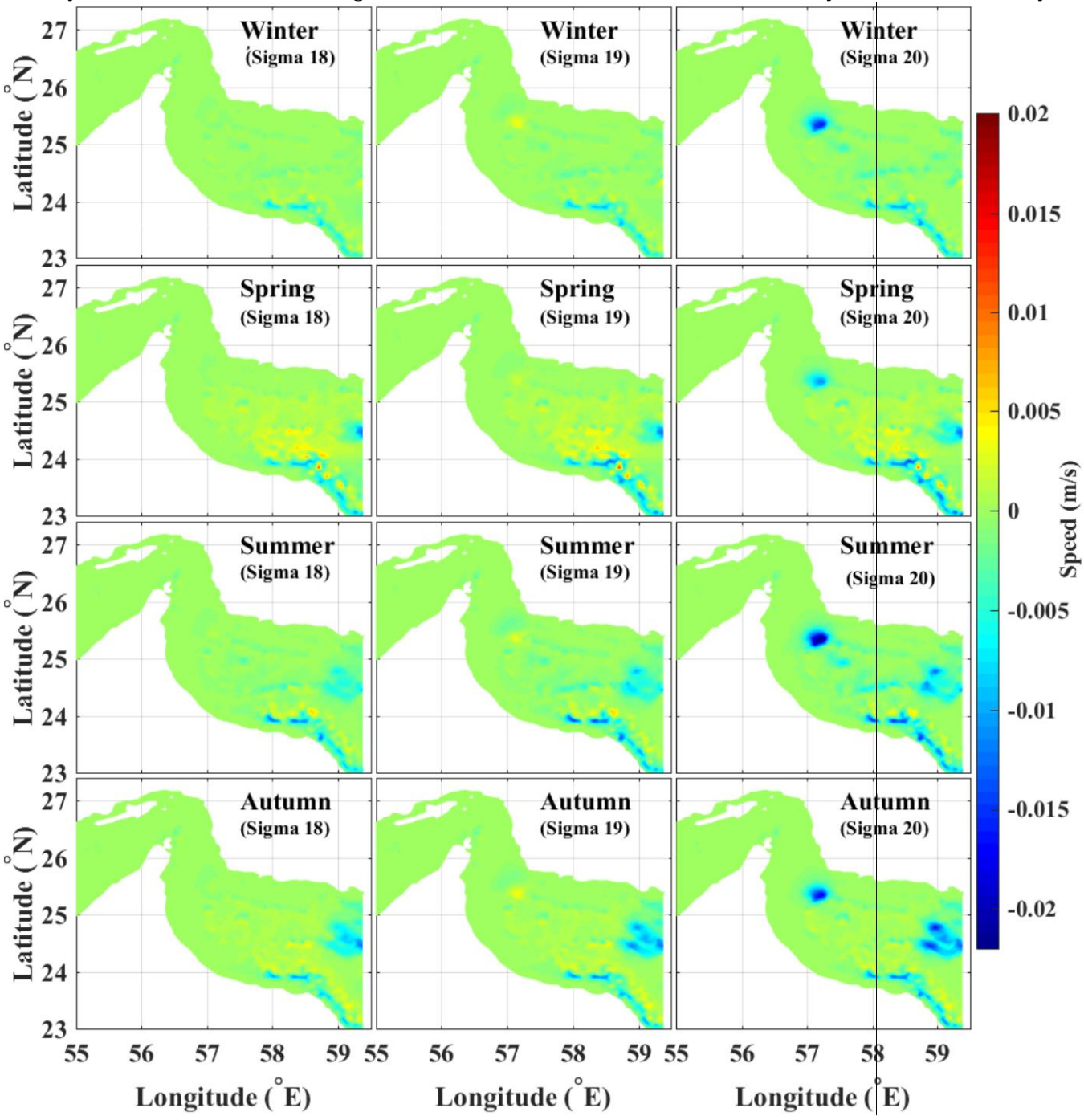

Figure 2. The water simulated vertical velocity in Gulf of Oman in winter, spring, summer and autumn, in last three layers near the bed (the first column: 18th, the second column: 19th, and the third column: 20th sigma layers, respectively). Positive values are upward and negative values are downward.

In autumn (the last row of figure 2) the vertical velocity of water in the 20th sigma layer is -0.2 cm/s to -0.1 cm/s in the Gulf of Oman and more than other areas in the longitude of 57.12˚E by the maximum value of -1.7

cm/s. In the eastern regions of the Gulf of Oman, in the longitude of 58.8˚E to 59.4˚E, the vertical velocity of water is about -0.8 cm/s to -1.7 cm/s, which is higher than other areas of this region. In the southern regions of the Gulf of Oman, there is a water strip that runs parallel to the coast and its velocity is -1.1 cm/s. In autumn, the downward vertical velocity is higher in the eastern regions of the study area than the other regions. In the 19th layer, the value of this speed in the east of the Gulf of Oman has reached 1.5 cm/s, which has increased compared to the summer and spring.

Overall, the east area of the Strait of Hormuz and the Gulf of Oman, the vertical velocity has more changes from latitude of 25.19˚N to 25.48˚N and longitude of 57.12˚E to 57.26˚E. The values of this velocity are -2cm/s in winter, -1 cm/s in spring, -1/2 cm/s in summer, and -1/7 cm/s in autumn. In the places where there is a sudden change in depth or the slope of the continental plateau, a downward velocity change, and the size of this speed is almost close to each other in all seasons. This sudden negative velocity change indicates downwelling in this area. This sinking of water is not caused by the surface wind tension, but it is the result of the change of the slope of the continental plateau. In all four seasons, as the depth increases from the 18th sigma layer to the 20th layer, the downward vertical velocity also increases. Therefore, the velocity shows that the outflow water of the Persian Gulf has entered the Gulf of Oman from near Jask Cape in the deep layer (yellow spots of sigma 19 in Figure 2).

Figure 3 shows the horizontal velocity of the 20th layer. In the areas where there was a downward vertical velocity value (56.9˚E to 57.25˚E), the horizontal velocity was also higher (red colors). It is -44 cm/s in winter, -32cm/s in spring, 70cm/s in summer and 60cm/s in autumn. In this area, there is a continental shelf break and a change in depth. In the surrounded areas, the flow velocity is lower (about 20 cm/s). In spring and autumn, in the eastern regions of the study basin (59 to 60˚E longitudes), the horizontal velocity is higher and its value reaches 30 cm/s. In a study that presented the general circulation of salinity in the Strait of Hormuz, the horizontal velocity of the dense water flow from the Persian Gulf to the Gulf of Oman was found to be 41 cm/s [31]. Another study [32] found the maximum velocity value for PGW flow in these areas to be 40 cm/s in summer and 55 cm/s in winter. Also, the speed of PGW in August and March was 35 cm/s and 69 cm/s, respectively [33]. The results of this study are in good agreement with the mentioned studies.

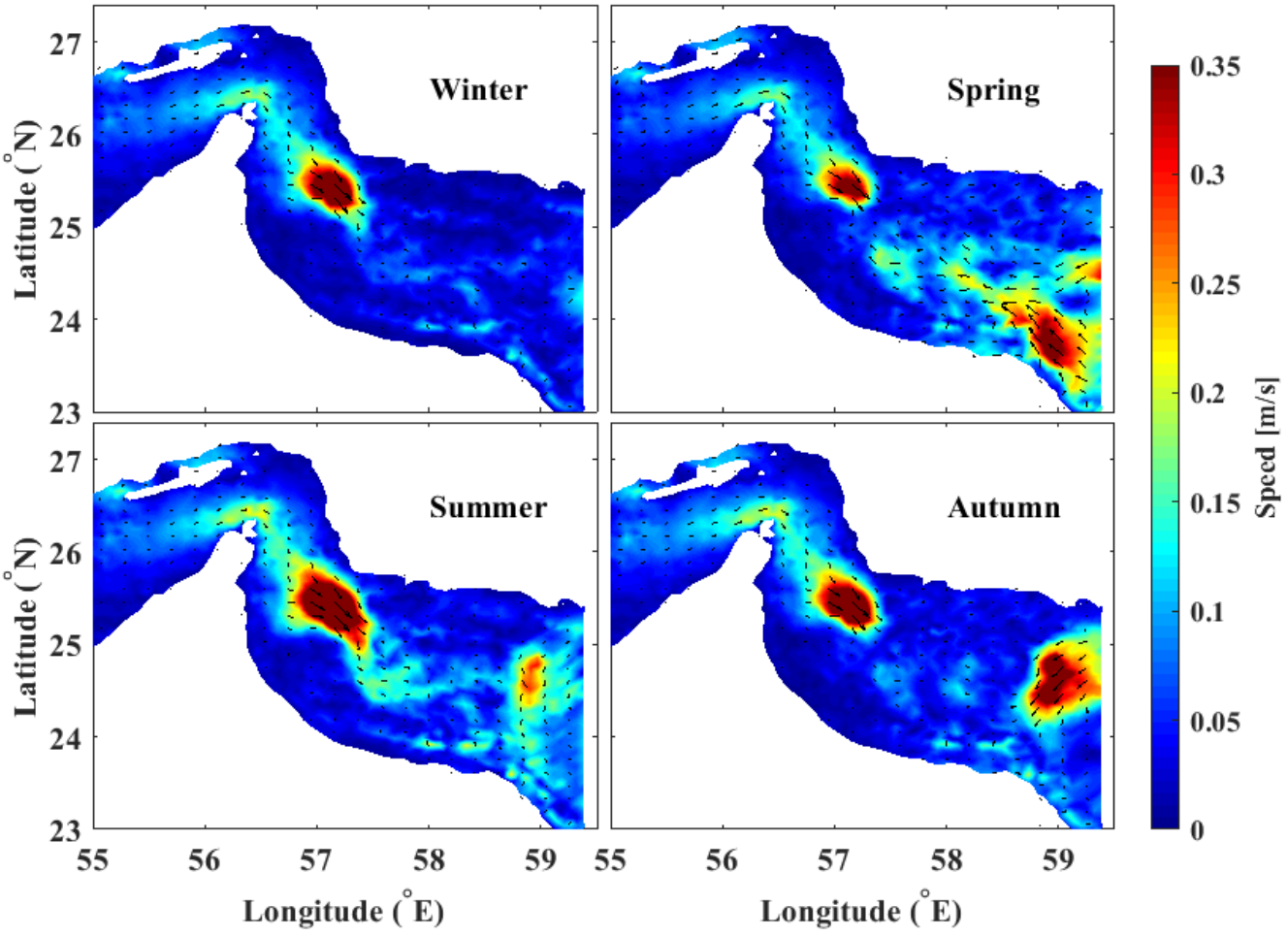

Figure 3. The simulation of the horizontal speed in the lowest layer (sigma=20) for winter, spring, summer and autumn.

It can be seen from Figure 4 that in winter, the eastern areas, which contain Gulf of Oman water entering to the Persian Gulf, have lower salinity (about 36.6 psu to 36.9 psu), and although in the western part, the surface

water has a salinity of 36.6 psu but in these areas, with increasing depth, the water salinity is increasing, and at depths more than 60 meters to 110 meters, the water salinity reaches between 37 psu and 37.8 psu (Figure 4, winter). The water salinity in the surface layer in spring is around 37.5 psu to 37.2 psu. The salinity more than 37.5 psu covers most of the deep water area in this season, which shows that the water with higher density has settled in the lower layers. (Figure 4, spring). In summer, the water in the eastern part is less saline, but in compared with winter, its salinity has increased. In the surface layers, the water salinity ranges from 36.5 psu to 37.2 psu, and in the western part, in the deep layers, the salinity is from 38 psu to 38.2 psu, which is the water outflow of the Persian Gulf (Figure 4, summer). In autumn, a saline water spot can be seen in the deep parts of the area, which indicates that water with more salinity has penetrated to the deep parts the same as winter (Figure 4, autumn).

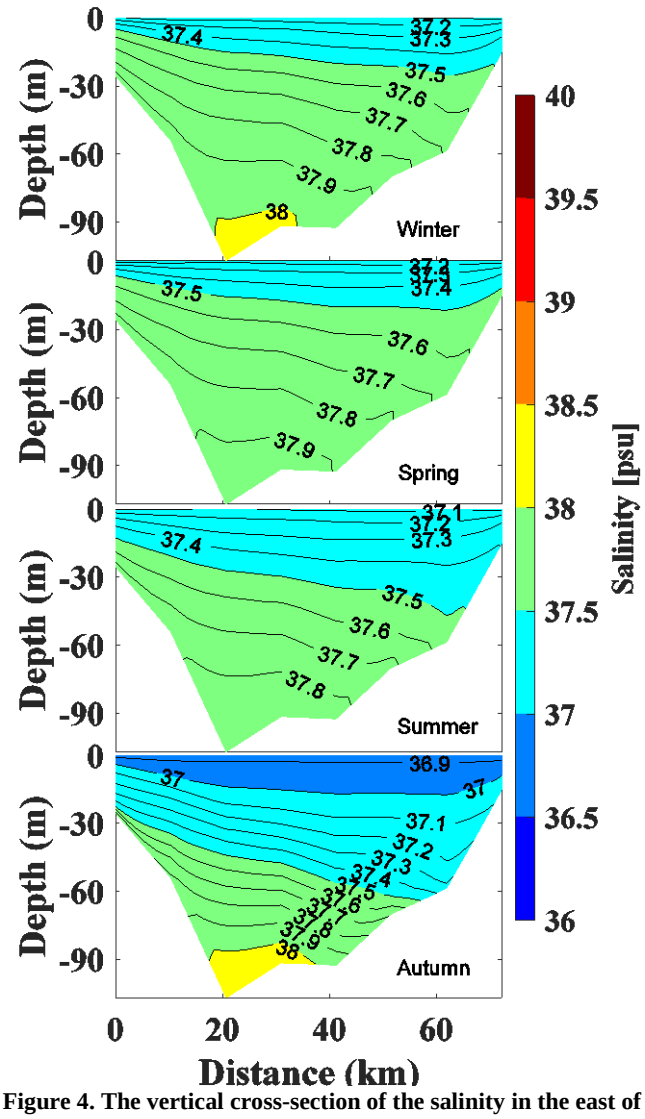

Figure 4. The vertical cross-section of the salinity in the east of the Strait of Hormuz in winter, spring, summer and autumn in section AA' (Figure 1).

The comparison of summer and winter from Figure 4 clearly shows the infiltration of salt water in winter season compared to summer. Figure 4 also shows the slope of the salt wedge exiting the Persian Gulf. The slope in Figure 4 is the boundary between cyan and light green color. It can be seen that these borders have different slopes in different seasons. In the summer, it can be seen that the color change occurs at a distance of about 60 kilometers (in the longitudinal direction) from a depth of 20 meters to a depth of 60 meters (40-meters differences in the vertical direction), that is, the calculated angle for this boundary is equal to 3.8×10^{-2} degrees. In the winter, at a horizontal distance of 40 kilometers from a depth of 20 meters to 80 meters (60-meters differences in the vertical direction), the color change is observed, that is, the angle calculated for winter slope is equal to 5.1×10^{-1} degrees. Although these angles are very small values, they are different for two seasons, summer (3.8×10^{-2} degrees) and winter (5.1×10^{-1} degrees). This fact indicates a stronger stratification of salinity in the summer season than in the winter season. Figure 4 also shows that in summer, the salinity contour lines are very close to each other, as a result, there is a stronger stratification in summer. In winter, the calculated slope is larger than summer, and the larger angle or the steeper slope (tangent of angle) of the boundry layer, the greater horizontal component of the water weight force ($mg\sin\theta$) that causes the water to move downward (Figure 5), and the water moves faster (Figure 5). According to this reasoning, the water in the Persian Gulf drains earlier and moves to lower depths sooner.

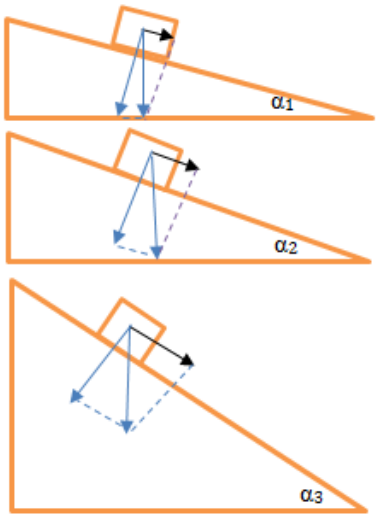

Figure 5. The comparison of the horizontal component of three water parcels placed on three different inclined surfaces with slopes α_1, α_2 and α_3 ($\alpha_1 < \alpha_2 < \alpha_3$).

The vertical section of temperature for the Strait of Hormuz for the seasons of the year is drawn in Figure 6. In winter, the water temperature of the surface layer is about 28°C, it is higher in the middle region, and lower in the western regions. The temperature of the lower layers decreases as the depth increases. In the lower layers, there is a larger volume of water in winter, with a lower temperature than summer, which shows that the outgoing mass, which has a higher salinity (Figure 4), has penetrated to deeper parts and indicates

the existence of the phenomenon of submergence in these areas (Figure 6). In spring, the water temperature in the western regions of the region is lower than other seasons (27.2°C) and a larger volume of water with a temperature of about 26.3°C is located in the middle layers. In summer, the surface water temperature is 30°C to 31°C, which decreases from east to west. In central areas, the water temperature is 30.4°C, and in the western part, from the surface to the depth, the water temperature decreases, and in the lower depths, the water temperature has reached 24.5°C (Figure 6, summer). In autumn, there is water with a temperature of 28°C in the surface layer, and water with a higher temperature (28.5°C) is also seen in middle areas, and with the depth increase, the temperatures of the lower layer decrease. The bed temperature reaches 26.7°C in autumn. A week stratification of temperature is also observed in autumn.

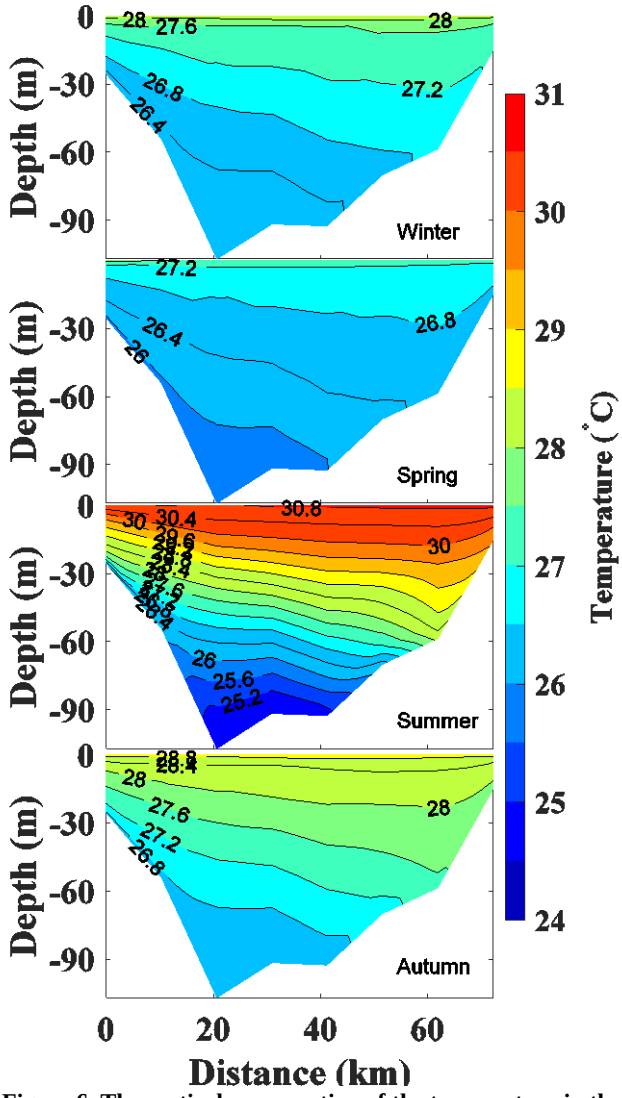

Figure 6. The vertical cross-section of the temperature in the east of the Strait of Hormuz in winter, spring, summer and autumn in section AA' (Figure 1).

This sinking of the saline water mass in winter mentioned in Figure 4 may be due to the lower temperature (Figure 6) and as a result, its higher density. It is expected that the movement of this warm and saline water mass will continue towards greater longitudes and greater depths, which is in good agreement with Khalilabadi (2015) [34]. Although many studies have shown the presence of Persian Gulf water in the Gulf of Oman [15-17, 20, 31-33, 35-38], the seasonal changes of its penetration in Gulf of Oman can be seen in [39-41]. Ramak et al., (2023) [41] showed that the Persian Gulf water mass with salinity (38.00 psu) flows out through the south of the Strait of Hormuz in the form of a subsurface flow in summer, and this water mass penetrates to greater depths and moves further away from the Strait of Hormuz in winter.

5. Conclusions

Investigating the seasonal changes of speed in this study clearly showed that an increase in speed can be seen in the lower layers. This increase of the speed for the deep layer (20th layer) and and a layer before the last layer (19th layer) is in opposite directions near Jask Cape. This fact indicates a two-way movement in the deep layers. The examination of temperature and salinity changes also showed that water infiltration in 25.19-25.48°N and 57.12-57.26°E is more in winter than all other seasons which indicates that more water sinks in these areas. This feature is in good agreement with other studies.

List of Symbols

E	Longitude [in ˚]
FVCOM	Finite-Volume Coastal Ocean Model
GHRSST	Group for High Resolution Sea Surface Temperature [in ˚C]
HYCOM	HYbrid Coordinate Ocean Model
N	Latitude [in ˚]
OSTIA	The Operational Sea Surface Temperature and Sea Ice Analysis
SMS	Surface-water Modeling System
TMD	Tidal Model Driver

8. References

[1] Brown E., Colling A., Park D., Phillips J., Rothery D., and Wright J. (2004), *Ocean Circulation*. 2nd ed. Boston Johannesburg: Jointly published by the Open University.

[2] Johannessen O.M., Subharaju G. and Blindhelm J. (1981), *Seasonal variation of the oceanographic conditions off the southwest coast of India during 1972-75*. Fiskeridirektoratets Skrifter Serie Havunders kelser, Vol.18, p.247-261.

[3] Mathew B. (1983), *Studies on upwelling and sinking in the seas around India*. University of Cochin, Cochin. PhD Thesis. p. 159

[4] Shetye S.R., Gouveia A.D., Shenoi S.S.C., Sundar D., Michael G.S., Almeida A.M., and Santanam K., (1990), *Hydrography and circulation off the west coast of India during the south-west monsoon 1987*. Journal of Marine Research, Vol.48(2), p.359-78.

[5] Hareesh Kumar P.V. and Basil M. (1997), *Salinity distribution in the Arabian sea.* Indian Journal of Marine Science, Vol.26(1), p.272-77.

[6] Mathew B., Sanilkumar K.V., Hareesh Kumar P.V., Madhusoodanan P. and James V.V. (1992), *Thermohaline and current structure off Cochin during December 1986*. Indian Journal of Marine Science, Vol.20, p.244-48.

[7] Zhou S., and Flynn P.C. (2005), *Geoengineering Downwelling Ocean Currents: A Cost Assessment*. Climatic Change. Vol.71, p.203–220. doi.org/10.1007/s10584-005-5933-0

[8] Sadrinasab M. (2009), *Three-dimensional numerical modeling study of the coastal upwelling in the Persian Gulf.* Research Journal of Environmental Science. Vol.3(5), p.560-566.

[9] McCreary J.P., Kundu P.K., and Molinari R.L. (1993), *A numerical investigation of dynamics, thermodynamics and mixed-layer processes in the Indian Ocean*, Progress in Oceanography, Vol.31(3), p.181–244, doi.org/10.1016/0079-6611(93)90002-U.

[10] Shetye S.R., Suresh I., Shankar D., Sundar D., Jayakumar S., Mehra P., Prabhudesai R.G., and Pednekar P.S. (2008), *Observational evidence for remote forcing of the West India Coastal Current*, Journal of Geophysical Research, Vol.113, p.C11001, doi.org/10.1029/2008JC004874.

[11] Shankar D. (1998), *Low-frequency variability of sea level along the coast of India*. PhD thesis, Goa University, Goa, India

[12] Shankar D., Vinayachandran P. and Unnikrishnan A.S. (2002), *The monsoon currents in the north Indian Ocean*. Progress in Oceanography, Vol.52, p.63–120.

[13] Shankar D., Remya R., Vinayachandran P.N., Chaterjee A., and Behera A. (2016), *Ihibition of mix-layer deepining during winter in the north-estern Arabian Sea by the west India Coastal Current.* Climate Dynamics, 47, 1049-1072. doi: 10.1007/s00382-015-2888-3.

[14] Vijith V., Vinayachandran P.N., Thushara V., Amol, P., Shankar D., and Anil A.C. (2016), *Consequences of inhibition of mixed-layer deepening bythe West India Coastal Current for winter phytoplankton bloom in the northeastern Arabian Sea*, Journal of Geophysical Research: Oceans, Vol. 121, p.6583–6603, doi:10.1002/2016JC012004.

[15] Pous S., Carton X., and Lazure P. (2004), *Hydrology and circulation in the Strait of Hormuz and the Gulf of Oman—Results from the GOGP99 Experiment: 1.Strait of Hormuz.* Journal of Geophysical Research Oceans. 109(C12). doi:10.1016/0016/2003JC002145 .

[16] Reynolds R.M. (1993), *Physical oceanography of the Gulf, Strait of Hormuz, and the Gulf of Oman—Results from the Mt Mitchell expedition*. Marine Pollution Bulletin. 27, 35-59.

[17] Soyufjahromi M. (2023). *The spatial and temporal monitoring of the sea surface temperature anomaly of the Strait of Hormuz*. International Journal Of Coastal and Offshore, And Environmental Engineering, accepted manuscripted. Available on line: 2023-01-16.

[18] Akbari P. Sadrinasab M. Chegini V. and Siadatmousavi M. (2016). *Tidal constituents in the Persian Gulf, Gulf of Oman and Arabian Sea: a numerical study*. Indian Journal of Geo-Marine Sciences. 45(8), 1010-1016.

[19] Soyuf Jahromi M. and Emami M. (2021). *The role of different positions of tidal turbines for energy extraction in Qeshm channel*. International Journal Of Coastal, Offshore And Environmental Engineering, 6(5), 1-9.

[20] Yao F. and Johns W.E. (2010), *A HYCOM modeling study of the Persian Gulf: 2. Formation and export of Persian Gulf Water*. Journal of Geophysical Research Oceans. 115(C11). doi:10.1029/2009JC005788.

[21] Chen C., Beardsley R., Cowles G., Qi J., Lai Z., Gao J., Stuebe D., Xu Q., Xue P., Ge J., Hu S., Ji R., Tian R., Huang H., Wu L., Lin H., Sun Y. and Zhao L. (2013), *An Unstructured Grid, Finite-Volume Community Ocean Model FVCOM User Manual*. FVCOM user manual, 416p.

[22] Chen C., Beardsley R.C. and Cowles G. (2006), *An unstructured grid, finite-volume coastal ocean model: FVCOM User Manual*. SMAST/UMASSD Technical Report-06-0602, University of Massachusetts-Dartmouth, New Bedford.

[23] Li B., Tanaka K.R., Chen Y., Brady D.C. and Thomas, A.C. (2017), *Assessing the quality of bottom water temperatures from the Finite-Volume Community Ocean Model (FVCOM) in the Northwest Atlantic Shelf region*. Journal of Marine Systems, 173, 21-30.

[24] IOC, IHO and BODC, (2003), *Centenary Edition of the GEBCO Digital Atlas, PUblished on CD-ROM on behalf of the Intergovernmental Oceanographic Commissioner and the International Hydrographic Organisation as part of the General Bathymetric Chart of the Ocean*. British Oceanographic data center, Liverpool.

[25] Brigham Young university, (2011), *SMS-Surface Water Modeling System Reference Manual Version 10*. Brigham young university-Enviromental Modeling Reference Laboratory, Provo, UT

[26] http://www.aquaveo.com

[27] http://www.gebco.net

[28] https://hycom.org

[29] The MathWorks Inc., (2016), *MATLAB and Statistics Toolbox 64-bit*, Version 2016a, Release 2016a, Natick, Massachusetts, USA.

[30] MetOffice, (2018), *The Operational Sea Surface Temperature and Sea Ice Analysis (OSTIA) system* https://www.ecmwf.int/sites/default/files/elibrary/2018/17975-operational-sea-surface-temperature-and-ice-analysis-ostia-system.pdf

[31] Thoppil P.G., and Hogan P.J., (2009), *On the mechanisms of episodic salinity outflow events in the Strait of Hormuz*. Journal of Physical Oceanography 39(6), 1340–1360.

[32] Bower A.S., Hunt H.D. and Price J.F. (2000), *Character and dynamics of the Red Sea and Persian Gulf outflows.* Journal of Geophysical Research: Oceans, 105(C3), 6387-6414.

[33] Ezam M., Bidokhti A.A. and Javid, A.H., (2010), *Numerical simulations of spreading of the Persian Gulf outflow into the Oman Sea*. Ocean Science., 6, 887–900, 2010.

[34] Khalilabadi M., (2015), *Three-dimensional simulation of water circulation in Oman Sea using MITgcm model*, Hydrophysics, Vol.2 (1), p.61-68.

[35] Johns, W. E., Yao, F., Olson, D. B., Josey, S. A., Grist, J. P., and Smeed, D. A. (2003). *Observations of seasonal*

exchange through the Straits of Hormuz and the inferred heat and freshwater budgets of the Persian Gulf. Journal of Geophysical Research: Oceans, Vol.108(C12).

[36] Azizpour J., Siyadat Mousavi Seyed Mostafa Siadat Mousavi S.M., and Chegini V. (2015). *Study of Physical Oceanographic Parameters in the Strait of Hormuz*, Hydrophysics, Vol.1(1), p.15-24.

[37] Ramak, H., Soyufjahromi, M., and Akbari, P. (2022). *Using surface temperature data of the Oman Sea to identify subsurface water of the Persian Gulf*. Hydrophysics, Vol.7(2), accepted manuscripted. Available on line: 2022-11-19.

[38] Ramak H, Soyufjahromi M, Akbari P. (2022). *Persian Gulf Water mass tracking by surface temperature and salinity properties*. Journal of Oceanography, Vol.12 (48), p.13-28.

[39] Ramak H, Soyufjahromi M, Akbari P. (2023). *Investigation of salinity and temperature of Persian Gulf water by FVCOM Model*. Journal of Oceanography, accepted manuscripted, 2022-11-19.

[40] L'Hégaret, P., Carton, X., Louazel, S., & Boutin, G. (2016). *Mesoscale eddies and submesoscale structures of Persian Gulf Water off the Omani coast in spring 2011*. Ocean Science, Vol.12(3), p.687-701.

[41] Ramek H, Soyufjahormi M, Akbari. P, (2023). *Investigation of physical properties of Persian Gulf water exchange using FVCOM Model*. Journal of oceanography, accepted manuscript 2022.